Optics Letters

Self-assembly of predesigned optical materials in nematic codispersions of plasmonic nanorods

Ghadah H. Sheetah,[1,2] Qingkun Liu,[1,2] and Ivan I. Smalyukh[1,2,3,4,*]

[1]Materials Science and Engineering Program, University of Colorado, Boulder, Colorado 80309, USA
[2]Department of Physics, University of Colorado, Boulder, Colorado 80309, USA
[3]Department of Electrical, Computer and Energy Engineering and Soft Materials Research Center, University of Colorado, Boulder, Colorado 80309, USA
[4]Renewable and Sustainable Energy Institute, National Renewable Energy Laboratory and University of Colorado, Boulder, Colorado 80309, USA
*Corresponding author: ivan.smalyukh@colorado.edu

Received 18 July 2016; revised 18 September 2016; accepted 21 September 2016; posted 22 September 2016 (Doc. ID 270800); published 20 October 2016

Optical metamaterials and other nanostructured metal-dielectric composites hold great potential for designing and practically realizing novel types of light–matter interactions. Here we develop an approach to fabricate composites with tunable pre-engineered properties via self-assembly of anisotropic nanoparticles codispersed in a nematic liquid crystal host. Orientations of plasmonic nanorods of varying aspect ratios are controlled to align parallel or perpendicular to the nematic director and retain this relative orientation during a facile electric switching. The ensuing dynamic reconfigurability of the surface plasmon resonances of a composite enables a previously inaccessible means of controlling light and may enable tunable plasmonic filters and polarizers.

OCIS codes: (160.3710) Liquid crystals; (250.5403) Plasmonics.

http://dx.doi.org/10.1364/OL.41.004899

Nematic liquid crystal (LC) colloids, formed by particles dispersed in a LC host fluid, provide a soft matter platform for designing novel composite materials with interesting optical properties [1–3]. This approach of designing mesostructured functional materials with novel physical behavior often combines unique optical properties of solid nanoparticles with long-range ordering and a facile response of the soft matter to weak external stimuli. The design and practical realization of diverse types of orientationally ordered nematic LC dispersions of nanoparticles is enabled by rich and highly complex LC-nanoparticle interactions on hierarchical scales, ranging from nanometers to device scales. The LC-mediated ordering of particles can emerge from elastic or surface-anchoring-based interactions, or a combination of both. Recent studies have demonstrated spontaneous self-alignment of nanoinclusions, such as rods, platelets, and topologically nontrivial colloidal objects [1–5]. However, despite the tremendous recent progress [6], the facile wet-chemistry-based synthesis approaches yield a limited variety of shapes and compositions of nanoparticles which, in turn, limits the prospects for the design of properties of nanoparticles dispersed within the ordered switchable composites.

In this Letter, we describe an approach of codispersing different anisotropic nanoparticles in LCs to design and realize composite materials with pre-engineered surface plasmon resonances (SPRs) and electrically tunable optical properties that could not be fabricated otherwise. To illustrate the power of this approach, we use rod-like gold nanoparticles of different aspect ratios and a different treatment of surfaces codispersed within the same nematic LC host. The nanorods of different types are controlled to align along the same direction of the nematic LC director **N** or in the mutually orthogonal directions, with one type of nanorods orienting parallel to **N** and the other type of rods orienting orthogonally to **N**. When low-voltage fields switch **N**, the nanorods are slave to changes of the **N**-orientation [2–4], rotating with their long or short nanorod axes mechanically coupled to **N** and, thus, enabling unprecedented tunability of SPR spectra and polarization-dependent optical properties of the ensuing composites. We characterize the threshold-like behavior of the electric switching of the composites, as well as the response times and other characteristics. We conclude with a discussion of potential practical uses of LC-nanoparticle codispersion composites in practical applications [7], such as tunable broadband polarizing elements and optical filters.

Aqueous dispersions of gold nanorods (GNRs) with mean diameters and lengths of 22 × 50 nm (short GNRs, SGNRs) and 21 × 80 nm (long GNRs, LGNRs) were synthesized using seed-mediated methods [8,9]. Before surface functionalization of GNRs aimed at defining boundary conditions (anchoring) for the LC molecules, the excess surfactant hexadecyltrimethylammonium bromide (CTAB, Sigma-Aldrich) initially used during synthesis of GNRs was removed. To define the tangential alignment of LC molecules and **N** on the surface of GNRs, we functionalized both SGNRs and LGNRs by thiol-terminated methoxy-poly(ethylene glycol) (mPEG-SH, JemKem Technology) [Fig. 1(a)] following the

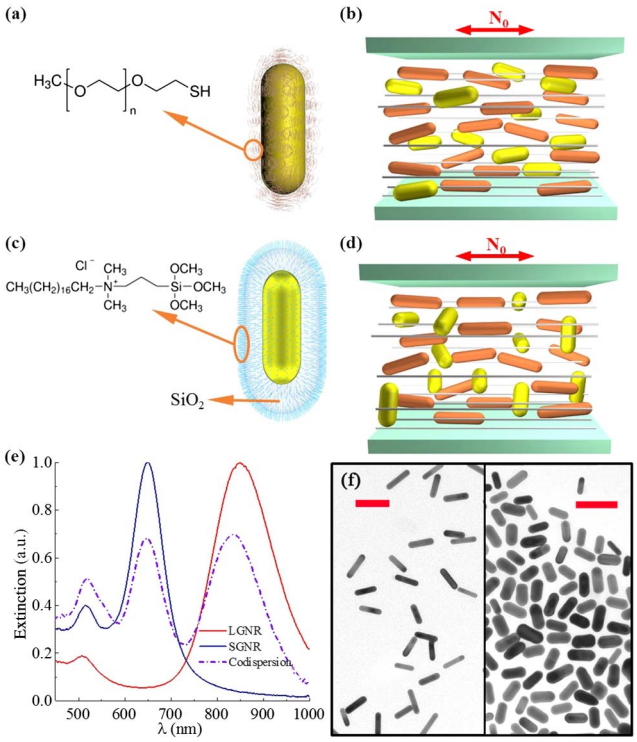

Fig. 1. Design of plasmonic nanocomposite materials and oriented self-assembly of codispersed GNRs. (a) Schematic of a GNR with the mPEG capping polymer layer on its surface. (b) Schematic of the codispersed GNRs with different aspect ratios, but treated to define the same tangential anchoring for **N** on their surfaces. (c) Schematic of a GNR with the silica coating and DMOAP capping layer on its surface. (d) Schematic of the codispersed GNRs with different aspect ratios that are treated to define different, tangential, or homeotropic surface anchoring for **N**. (e) Extinction spectra of both SGNRs and LGNRs when separately and jointly dispersed in an isotropic solvent (ethanol) at a dilute total concentration of 0.6 wt. %. (f) TEM images of the long (left) and short (right) GNRs; the red scale bars are 100 nm.

literature [4]. To achieve the homeotropic anchoring of LC molecules and **N** on the GNR surface, SGNRs were first capped with 10 nm thick mesoporous silica and then surface-functionalized by N,N-dimethylN-octadecyl-3-aminopropyltrimethoxysilyl chloride (DMOAP, 60% in methanol, from Acros Organics) [Fig. 1(c)] [3,10]. Briefly, 50 μL of a 0.1 M aqueous NaOH solution were added (under vigorous stirring) to a 5 mL of aqueous dispersion of GNRs with an optical density (OD) of 4.7 and 1.1 mM CTAB. Then 700 μL of 0.25 vol. % tetraethyl orthosilicate (Sigma-Aldrich) in ethanol were added with gentle stirring for 0.5 h and were kept undisturbed for 14 h. After washing with centrifuging twice, 4 mL of GNR solution with an OD of 2.3 was diluted to 8 mL; then 400 μL of DMOAP were injected under stirring. The solution was kept stirred for 20 min and washed by repeated centrifugation and transferred into methanol. Capped GNRs were redispersed in methanol and mixed with a nematic 4-cyano-4′-pentylbiphenyl (5CB, from Chengzhi Yonghua Display Materials Co. Ltd.), followed by full evaporation of the solvent at 90°C. The mixture was sonicated for 5 min at 40°C and cooled down to the nematic phase while vigorously stirring, yielding excellent dispersion in the LC phase at a high concentration. The codispersion of SGNRs and LGNRs with designed cappings was obtained by mixing them as dispersions with comparable ODs. LC cells were constructed from 0.17 or 1.0 mm thick glass substrates coated with transparent indium tin oxide electrodes and polyvinyl alcohol (PVA) alignment layers. Their inner surfaces with PVA layers were unidirectionally rubbed to impose the planar surface boundary conditions for the far-field director $\mathbf{N_0}$ parallel to the rubbing direction. The LC-nanoparticle composite was sandwiched between two such plates, with the cell gap defined by silica beads or Mylar spacers of corresponding diameters/thicknesses. Capillary action was used for the cell filling with the composite colloidal dispersion. UV-curable glue NOA-65 (Norland Products, Inc.) was used to bind the substrates together and to seal the cell edges.

We used Olympus BX-51 polarizing optical microscope equipped with 10×, 20×, and 50× air objectives with a numerical aperture NA = 0.3–0.9 and a charge coupled device camera Spot 14.2 Color Mosaic (Diagnostic Instruments, Inc.). Extinction spectra were studied using a spectrometer USB2000-FLG (Ocean Optics) mounted on the microscope and an Integrating Sampling System (ISS-2, Ocean Optics) as a light source. The polarized SPR spectra were measured by having light pass through the LC cell and then through a broadband (400–1200 nm) rotatable polarizer. Dark field imaging utilized an oil-immersion dark-field condenser (NA = 1.2), so that only highly scattered light was detected. Electric switching of codispersions was characterized using a data acquisition system SCC-68 (National Instruments Co.) controlled by homemade software written in Labview (National Instruments Co.) and a Si-amplified photodetector PDA100A (Thorlabs Inc.). Our selective studies of switching of different GNRs in LC were done in the vicinity of their longitudinal SPR wavelengths and utilized bandpass optical interference filters procured from Semrock Inc. Transmission electron microscopy (TEM) images were obtained using a CM100 microscope (FEI Philips).

Since the wet chemical synthesis and other means of facile fabrication of metal nanostructures provide only limited control of the ensuing SPR properties [6,7], colloidal self-assembly of simple-shape nanoparticles (such as spheres, rods, and platelets) into more complex plasmonic nanostructures has been broadly considered as a means to mitigate these limitations [7–13]. The enrichment of the SPR effects could be achieved through the coupling of SPR modes of individual nanoparticles upon their assembly into clusters, crystals, and other colloidal superstructures [7–13]. However, these approaches are typically limited to colloidal self-assemblies with nanoparticles at distances comparable to their dimensions. In dilute nanoparticle dispersions, such control is limited. Although multiple types of plasmonic nanoparticles, such as GNRs with different aspect ratios (Fig. 1), can be codispersed in isotropic fluid hosts [Fig. 1(e)], the extinction spectra of such dilute codispersions are usually just superpositions of those due to the individual constituent nanoparticle dispersions with a very limited ability of controlling them. In this Letter, we use an example of codispersions of LGNRs and SGNRs in a nematic host to demonstrate that spontaneous predesigned self-alignment of either long [Fig. 1(b)] axes or short and long axes [Fig. 1(d)] of SGNRs and LGNRs with the LC director **N** allows us to pre-engineer the ensuing composite medium's optical properties

through exploiting the polarization-dependent SPR resonances of aligned nanoparticles.

SGNRs and LGNRs functionalized by mPEG self-align with their long axes roughly parallel to **N** [Fig. 1(b)]. This spontaneous alignment is reminiscent to that of individual dispersions of SGNRs and LGNRs in LCs [2] and is driven by minimization of the surface anchoring free energy due to the finite-strength tangential boundary conditions on nanoparticle surfaces. Polarizing optical microscopy [Figs. 2(a) and 2(b)] shows that GNRs do not perturb the uniform alignment of the LC host while dispersed at rather high concentrations up to 1.6 wt. %. Dark field imaging [Fig. 2(c)] of the SGNR and LGNR codispersion in the aligned LC reveals Brownian

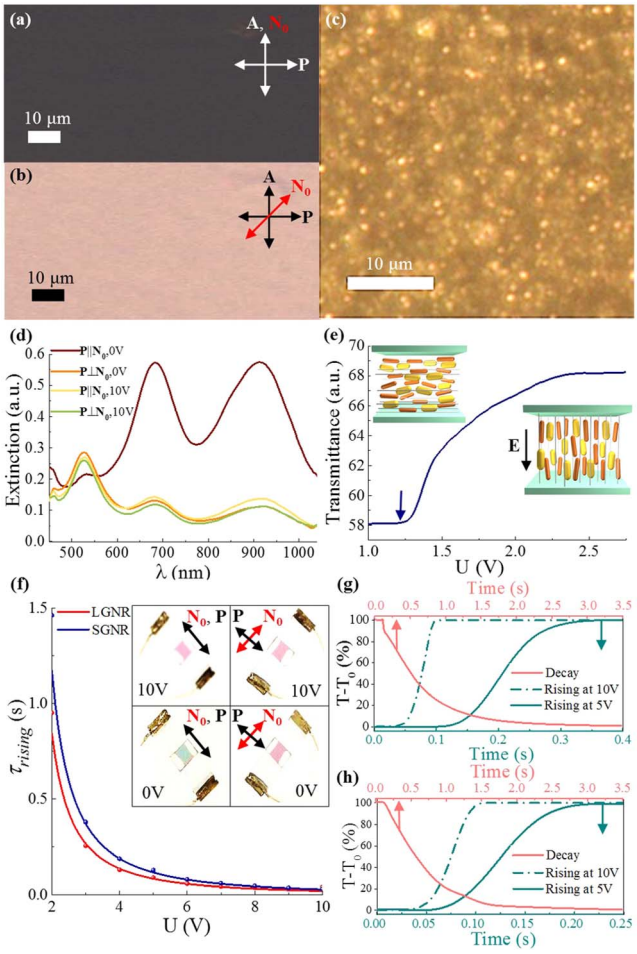

Fig. 2. Codispersion, coalignment, and switching of like-anchored GNRs in a nematic LC. (a), (b) Polarizing optical micrographs of a planar cell with $\mathbf{N_0}$ (a) parallel to analyzer (**A**) and (b) at 45° to a crossed polarizer (**P**) and **A**. (c) Dark field micrograph of a cell with $\mathbf{N_0}$ along its horizontal edge. (d) Polarized extinction spectra of the cell for linear polarizations $\mathbf{P}\|\mathbf{N_0}$ and $\mathbf{P}\perp\mathbf{N_0}$ at no applied fields and at applied voltage $U = 10$ V. (e) Voltage dependence of transmittance of white light polarized along the rubbing direction measured using a microscope, with the threshold voltage marked by an arrow. (f) Voltage-dependent rising time for both types of GNRs. The insets show photographs of the inch-size cells at different orientations of $\mathbf{N_0}$ relative to **P**. (g), (h) Rising and decay times for (g) SGNR and (h) LGNR dispersions measured based on relative changes of transmittance (T-T_0) for the same codispersion sample by using optical bandpass filters corresponding to their longitudinal SPRs. The cell thickness is 30 μm.

motion of the nanoparticles on an individual basis, without forming aggregates, which was assessed on the basis of their diffusion [5]. Polarized extinction spectra have three peaks, one corresponding to the transverse SPR modes at ≈530 nm of both SGNRs and LGNRs and two peaks corresponding to the spectrally separated longitudinal SPR modes of the two types of nanorods. When the effects of a relatively high polarization-dependent effective refractive index of the LC host are accounted for, the spectral locations of all SPR peaks [Fig. 2(d)] appear consistent with those of the same GNRs in an isotropic host [Fig. 1(e)]. In a planar cell, the extinction spectra exhibit strong dependencies on the polarization of light **P** and applied AC voltage U (at 1 kHz), with the maximum extinction values at $\mathbf{P}\|\mathbf{N_0}$ corresponding to the two longitudinal SPR modes of the constituent GNRs. At $\mathbf{P}\perp\mathbf{N_0}$, an extinction peak is located at the transverse SPR mode wavelength [Fig. 2(d)]. The voltage dependence of light transmission through the cell exhibits a threshold-like behavior [Fig. 2(e)], showing no or little change up to a threshold voltage U_{th} and then changing dramatically with the increase of U. This behavior is consistent with the U-dependent extinction spectra [Fig. 2(d)] and the synchronous field-induced realignment of **N** and GNRs schematically shown in the insets of Fig. 2(e). Since the longitudinal SPR modes are polarized along the long axes of the nanorods, the extinction spectra allow us to determine the scalar order parameters (defined as $S_{\text{GNR}} = \langle 3\cos^2\theta_{\text{GNR}} - 1\rangle/2$) characterizing the orientational order of both SGNRs and LGNRs. Using the peak extinction values $A_{\|}$ and $A_{\perp}$ of longitudinal SPR for $\mathbf{P}\|\mathbf{N_0}$ and $\mathbf{P}\perp\mathbf{N_0}$ and a relation $S_{\text{GNR}} = (A_{\|} - A_{\perp})/(A_{\|} + 2A_{\perp})$, we find that the order of GNRs is characterized by $S_{\text{LGNR}} = 0.58$ and $S_{\text{SGNR}} = 0.50$, respectively.

The kinetics of electric switching of SGNRs and LGNRs is probed by using bandpass filters matching their longitudinal SPR peaks. The rising and decay times are found from relative changes of the transmitted light intensity between 10% and 90% with respect to their maximum and minimum values. The switching times of GNRs in the nanorod-LC codispersion are comparable to those of the pristine LCs, with the rising (voltage-on) times dependent on U, albeit the reorientation of LGNRs is slightly faster than that of SGNRs [Figs. 2(f)–2(h)]. This could be due to the relative strengths of mechanical coupling between **N** and the orientations of GNRs, which is stronger for LGNRs, consistent with $S_{\text{LGNR}} > S_{\text{LGNR}}$. The decay times (response to voltage off) are also comparable to what one expects for cells of a pristine LC with the same thickness $d = 30$ μm [2]. The measured response time values [Figs. 2(g) and 2(h)] qualitatively agree with the theoretical prediction for pristine LCs $\tau_{ri\,\sin g} = \tau_{\text{decay}}/[(U/U_{\text{th}})^2 - 1]$, where $\tau_{\text{decay}} = \gamma_1 d^2/(K_{33}\pi^2)$ is the decay time, γ_1 is the rotational viscosity, and K_{33} is the bend elastic constant. The insets of Fig. 2(f) show that the polarization dependence of the composites can be controlled in the same way over the large areas of the cells (demonstrated for inch-size cells, but can be scaled to meters, as long as the LC host can be aligned).

Figure 3 shows a very different behavior of a codispersion of DMOAP-functionalized silica-coated SGNRs [inset of Fig. 3(a)] and mPEG-functionalized LGNRs in the same 5CB LC host. The homeotropic and tangential boundary conditions on the SGNR and LGNR particle surfaces prompt their self-alignment perpendicular and parallel to $\mathbf{N_0}$, respectively [Fig. 1(d)], again driven by the minimization of the surface

anchoring energy [2,3]. As the polarization of probing light is switched between $\mathbf{P}\|\mathbf{N_0}$ and $\mathbf{P}\perp\mathbf{N_0}$, the longitudinal SPR peaks due to the two GNRs alternate while varying between maximum and minimum values of extinction at the corresponding wavelengths. The finite S_{GNR}–values characterizing the LC-induced order of both GNRs manifest themselves in that the longitudinal peaks of the two rods never disappear with rotating $\mathbf{P}$. Using the same approach as that of the tangentially anchored rod codispersion, we determine the scalar order parameters to be $S_{LGNR} = 0.65$ and $S_{SGNR} = -0.31$, respectively. The polarized SPR spectra can be also controlled by applying voltage while switching $\mathbf{N}$ and having the orientation of $\mathbf{P}\|\mathbf{N_0}$ fixed [Fig. 3(b)]. Both the alignment and switching can be controlled on centimeter square areas of the LC cells [insets of Fig. 3(c)]. This can be extended to a much larger LC cell dimensions, such as that of large-screen TVs.

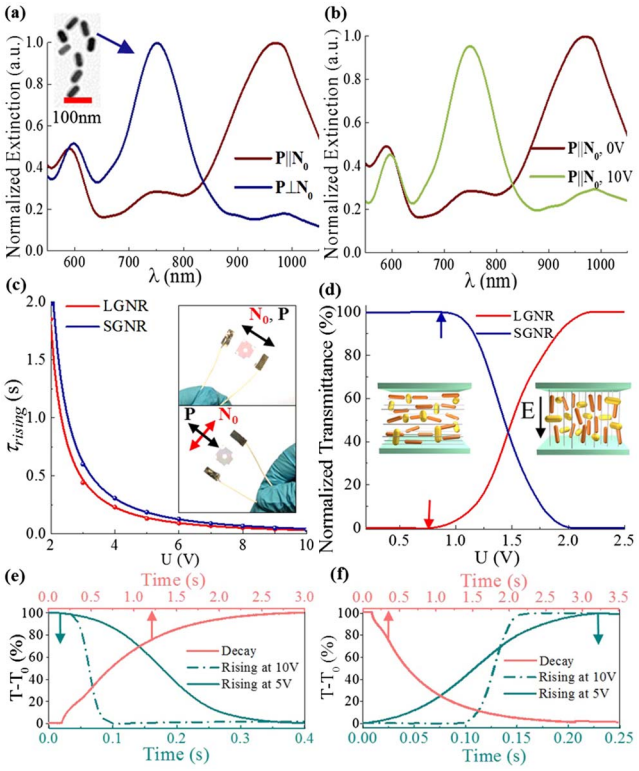

Fig. 3. Codispersion, coalignment, and switching of differently anchored GNRs in a nematic LC. (a) Normalized extinction of a codispersion of LGNRs treated for tangential and SGNRs treated for perpendicular anchoring for $\mathbf{P}\|\mathbf{N_0}$ and $\mathbf{P}\perp\mathbf{N_0}$. The inset is a TEM image of the silica-coated SGNRs. (b) Switching of the extinction spectra at $\mathbf{P}\|\mathbf{N_0}$ by applying $U = 10$ V. (c) Voltage-dependent rising times for both types of GNRs codispersed in the same LC sample, along with photographs of the cell (30 μm thick, square-inch area filled with the codispersion) in the inset showing the change of color upon changing polarizer orientation from $\mathbf{P}\|\mathbf{N_0}$ (top) to $\mathbf{P}\perp\mathbf{N_0}$ (bottom). (d) Voltage dependence of light transmission at the longitudinal wavelengths of SGNRs and LGNRs, with the threshold voltages marked by colored arrows. The insets are schematics of the cell before and after applying U much larger than U_{th}, along with the schematically shown alignment of particles in the LC with and without applied U. (e), (f) Rising and decay times for (e) SGNRs and (f) LGNRs measured based on the relative changes of transmittance T-T_0 for the same LC codispersion by using optical bandpass filters corresponding to their longitudinal SPRs.

The threshold-like switching of the cells [Fig. 3(d)] manifests itself very differently when probed separately at the wavelengths of longitudinal SPR modes of the two GNRs. The transmitted intensity at the SGNR's longitudinal SPR mode wavelength stays intact with increasing U up to U_{th}, but then decreases continuously above it [Fig. 3(d)]. The transmitted intensity at the LGNR's longitudinal SPR peak wavelength stays intact with increasing U up to U_{th}, but then increases continuously at $U > U_{th}$ [Fig. 3(d)]. This behavior is consistent with the switching of $\mathbf{N}$ from its initial in-plane orientation to the vertical orientation and the ensuing realignment LGNRs and SGNRs that maintain their orientations relative to U-controlled $\mathbf{N}$ [insets of Fig. 3(d)]. Interestingly, U_{th} is slightly lower than that measured for the codispersion with both LGNRs and SGNRs aligned along $\mathbf{N}$ [Fig. 2(e)]. The time response characteristics [Figs. 3(e) and 3(f)] are qualitatively consistent with those of pristine LCs and the plasmonic guest-host LCs, albeit the response times for SGNRs being slower than for LGNRs.

The above examples based on SGNRs and LGNRs demonstrate that anisotropic plasmonic nanoparticles can be aligned in LC host fluids so that the polarized plasmonic modes of these nanoparticles have different orientations with respect to each other and the LC director. By varying the aspect ratios, composition (e.g., some particles could be made of silver while others of gold), and geometric shape of individual types of codispersed particles in the composite, one can tune both the locations of SPR peaks and their polarization-dependent properties as needed for the design of optical materials.

To conclude, we have demonstrated an approach of predesigned control of optical properties of plasmonic mesostructured nanoparticle-based composites, which involves the alignment of polarized SPR modes of nanoparticles with different shapes and compositions codispersed within an ordered LC host. Our findings open new possibilities for engineering the physical behavior of self-assembled optical metamaterials, as well as technological uses in plasmonic nanolasers, guest-host LC displays and smart windows [2], and electrically switchable broadband polarizing elements and tunable optical filters.

REFERENCES

1. Q. Liu, Y. Cui, D. Gardner, X. Li, S. He, and I. I. Smalyukh, Nano Lett. **10**, 1347 (2010).
2. Q. Liu, Y. Yuan, and I. I. Smalyukh, Nano Lett. **14**, 4071 (2014).
3. Y. Zhang, Q. Liu, H. Mundoor, Y. Yuan, and I. I. Smalyukh, ACS Nano **9**, 3097 (2015).
4. Y. Yuan and I. I. Smalyukh, Opt. Lett. **40**, 5630 (2015).
5. B. Senyuk, D. Glugla, and I. I. Smalyukh, Phys. Rev. E **88**, 062507 (2013).
6. S. Link, Z. L. Wang, and M. A. El-Sayed, J. Phys. Chem. B **103**, 3529 (1999).
7. H. K. Bisoy and S. Kumar, Chem. Soc. Rev. **40**, 306 (2011).
8. J. Perez-Juste, L. M. Liz-Marzan, S. Carnie, D. Y. C. Chan, and P. Mulvaney, Adv. Funct. Mater. **14**, 571 (2004).
9. X. Ye, L. Jin, H. Caglayan, J. Chen, G. Xing, C. Zheng, V. Doan-Nguyen, Y. Kang, N. Engheta, C. R. Kagan, and C. B. Murray, ACS Nano **6**, 2804 (2012).
10. W. C. Wu and J. B. Tracy, Chem. Mater. **27**, 2888 (2015).
11. J. A. Fan, C. Wu, K. Bao, J. Bao, R. Bardhan, N. J. Halas, V. N. Manoharan, P. Nordlander, G. Shvets, and F. Capasso, Science **328**, 1135 (2010).
12. M. R. Jones, R. J. Macfarlane, B. Lee, J. Zhang, K. L. Young, A. J. Senesi, and C. A. Mirkin, Nat. Mater. **9**, 913 (2010).
13. T. Hu, B. P. Isaacof, J. H. Bahng, C. Hao, Y. Zhou, J. Zhu, X. Li, Z. Wang, S. Liu, C. Xu, J. S. Biteen, and N. A. Kotov, Nano Lett. **14**, 6799 (2014).